JOURNAL OF PROPULSION AND POWER
Vol. 11, No. 2, March–April 1995

Acoustic Control of Combustor Primary Zone Air-Jet Mixing

P. J. Vermeulen,* V. Ramesh,† and B. Sanders‡
University of Calgary, Calgary, Alberta T2N 1N4, Canada
and
J. Odgers§
Université Laval, Quebec G1K 7P4, Canada

A small tubular combustor of conventional gas turbine design and behavior, employing acoustically controlled primary zone air-jet mixing processes, has been successfully tested at scaled one-fourth-load operating conditions, and some data were obtained at one-half and three-quarter loads. The acoustic drive produced a more uniform exit plane temperature pattern, resulting in up to 35% improvement in mixing relative to no-drive, and up to 20% relative improvement in the temperature pattern quality. The effects depended on air/fuel ratio, and in general, improved relative to no-drive with richening. At three-quarter load, 150-W single-driver power, the acoustic driving effectiveness was reduced by about 80% with correspondingly reduced improvements in mixing and quality. The effects of acoustic drive were favorably controlled by means of the driving power, and increased flow blockage caused by increased jet penetration by the acoustic drive appears to be the control mechanism.

Nomenclature

A/F = air/fuel ratio, by mass flow rate
D = jet orifice diameter
f = driving frequency
$\dot{M}$ = mass flow rate
M_r = reference Mach number based on maximum i.d. of casing
n = number of data points
p = static pressure
p_0 = stagnation pressure
Q = exit temperature pattern quality
R = residual temperature standard deviation
S_m = mixing standard deviation calculated for all data of set
S_p = temperature profile acoustic driving effectiveness calculated for all data of set
St = jet Strouhal number at the orifice, fD/U_j
T = local average stagnation temperature, ≅ local average static temperature
$\bar{T}_{3m}$ = average value of T_{3m} no-drive and T_{3m} with-drive
$(T_3)_0$ = exit plane local average temperature at 0-deg thermocouple array position
$(T_3)_{360}$ = exit plane local average temperature at 360-deg thermocouple array position
U_e = jet velocity excitation pulsation amplitude, at the orifice exit plane center (unsteady flow)
U_j = steady mean jet velocity at the orifice exit plane
$\dot{W}$ = power at acoustic driver
θ_m = local average dimensionless relative temperature
ρ_j = density of the jet flow at orifice exit plane

Subscripts

a = air
f = fuel
m = mean
max = maximum
ND = no drive
t = calculated for truncated data set
WD = with drive
2 = inlet plane, T_2 at centerline
3 = exit plane

Received Oct. 17, 1992; revision received June 27, 1994; accepted for publication June 27, 1994.

*Professor, Department of Mechanical Engineering. Member AIAA.
†Research Associate, Department of Mechanical Engineering.
‡Research Technician, Department of Mechanical Engineering.
§Professor Titulaire, retired, Département de Génie Mécanique. Member AIAA.

Introduction

SATISFACTORY gas turbine combustor performance depends critically on good air-jet mixing.[1] For instance, in the primary zone, high burning rates and minimum soot and nitric oxide formation are attained by good mixing. In the dilution zone the thorough mixing of dilution-air and combustion products is necessary for a satisfactory temperature pattern quality at the combustor exit. Acoustically excited jets give superior mixing properties over steady jets, therefore, the technique has been applied to the air-jets of the combustor primary zone because of the potential for control and improvement in combustor performance.

The earliest known work on acoustically excited jets is that of Hahnemann and Ehret[2] in 1943 who modulated a propane-air mixture flowing to a nozzle burner and showed that the flame shape was strongly modified. The stability of acoustically excited jets was studied by Refs. 3–6, who showed that there are two main instability modes. In the first mode the initial thin laminar boundary layer develops waves before rolling up into toroidal vortices on progression along the jet. A turbulent boundary layer cannot sustain oscillations, but the jet column can, and on excitation develops wave motion growing into a train of toroidal vortices as the second mode. At optimum or strong driving conditions the vortices are strong enough to disintegrate the jet column. Air-jets have been harmonically excited up to 20 kHz, up to a Mach number of 0.6, and for Reynolds numbers up to 10^6, to establish toroidal vortices.[7,8]

The majority of work on the excited jet has been concerned with jet noise and turbulence, and little attention was given to jet mixing. However, from the indirect measurement of integrating velocity profiles, Crow and Champagne,[5] Binder and Favre-Marinet,[9] Hill and Greene,[10] and Bremhorst and Harch,[11] established that the entrainment rate could be increased by as much as 90%. Following on this, Vermeulen et al.[12,13] established that the dilution-air-jet mixing processes of a small tubular combustor of conventional gas turbine design could be beneficially controlled by acoustic means. This work

showed that acoustic excitation of the dilution-air-jet flows allowed selective and progressive control of the exit plane temperature distribution. In particular, for an already good temperature traverse quality, it was possible to trim the temperature profile. Thus, by these means a desired exit-plane temperature distribution may be achieved. From these results it was inferred that the entrainment rate and mixing of the dilution-air-jets was increased by the acoustic pulsations. These encouraging results promoted detailed investigations into acoustically pulsed freejet mixing,[14-16] and showed that the entrainment and entrainment coefficient of the jet could be considerably increased, by up to six times. Therefore, jet mixing would be improved also, since jet entrainment is responsible for the mixing produced by a jet.

Gas turbine combustor performance depends in particular on the mixing of air-jets with a confined hot crossflow. Therefore, experimental studies were done on an acoustically pulsed air-jet mixing with a confined crossflow,[17,18] and showed that mixing was significantly increased, and penetration at least 100% increased. The entraining action of the traveling toroidal vortices is the primary mechanism of the acoustically augmented mixing and penetration processes. The response of the acoustically pulsed jet, as determined from penetration and mixing, was found to be optimum at a *St* of about 0.27.

The novel experiments on acoustic control of combustor primary zone air-jet mixing to be reported were designed to examine the effectiveness and control by the acoustic drive, by means of temperature profile measurements in the combustor exit plane, over representative ranges of air/fuel ratio, reference Mach number, and acoustic driver power.

Experimental

Combustor with Acoustically Pulsed Primary Zone Air-Jets

The apparatus is essentially the same as that described in Refs. 12 and 13, except that the combustor exit plane (87.63 mm i.d.) temperature distribution is now measured by 18 shielded thermocouples in a 3-spoked array, which was rotated in 15-deg steps to produce a polar data array of 432 temperature measurements. Figure 1[12] shows a cross section of the combustor, unmodified for acoustic control, giving its air distribution and important features. Provision was made for the measurement of air and fuel mass flow rates and the combustor inlet and exit conditions. Thermocouples attached to the outside wall of the flame tube measured wall temperatures in the primary and dilution zones. The pressure and temperature data obtained were processed by a PC-controlled data logging system, and exit plane temperature distributions were analyzed by a Sun mainframe computer.

Figure 2 illustrates the method for acoustic control of the conventional gas turbine tubular combustor primary zone. The usual liquid fuel atomizer has been replaced by a conical gas injector for the burning of commercial natural gas. The method channels air from upstream of the combustor inlet via 6 bypass tubes connecting to a split manifold of 3 separate segments, which feeds the 20 primary zone air-jet holes in the flame tube. Ten pairs of radial tubes cross the combustor annulus to connect the air holes of the flame tube to the manifold segments surrounding the combustor casing. Each manifold segment is connected by a driver tube to a 300-W loudspeaker that provides the acoustic driving and control. The strongest acoustic driving mode of the system was established by means of an HP 5423A two-channel analyzer, using a voltage proportional to the loudspeaker current, as an input signal and the voltage from a microphone measuring sound pressure near the exit of a primary zone air-jet hole in the flame tube as an output signal. These measurements were made without airflow through the combustor. However, to check that the measurements were meaningful, a hot-film anemometer was used to measure the air-jet velocity through a primary zone hole for a modest airflow through the combustor. Under acoustic drive conditions, the anemometer detected the strongest pulsating flow at the strongest acoustic mode of the system, thereby confirming that the no-flow analysis was meaningful, and that the optimum acoustic test frequency was 227 Hz. Because of limited funding, a single two-channel amplifier powered the three loudspeakers, thereby necessitating a parallel connection for two speakers when all three speakers were being used simultaneously. Power at a loudspeaker driver was measured by an a.c. voltmeter and ammeter, ignoring the power factor since previous work had shown it to be close to unity.[15]

Table 1 summarizes the range of test conditions used and indicates that up to scaled three-quarter-load operation, based upon the reference Mach number aerodynamic scaling factor, was achieved. As is usual for this type of combustor, M_r was calculated at the maximum i.d. of the casing (142.9 mm diam).

Combustor Measurements and Accuracy

The thermocouples measuring the exit plane temperature distribution were arranged so that seven thermocouples measured the temperature of seven equal area zones. The 11 remaining thermocouples were then arranged so that well-defined diametral temperature profiles would be measured,

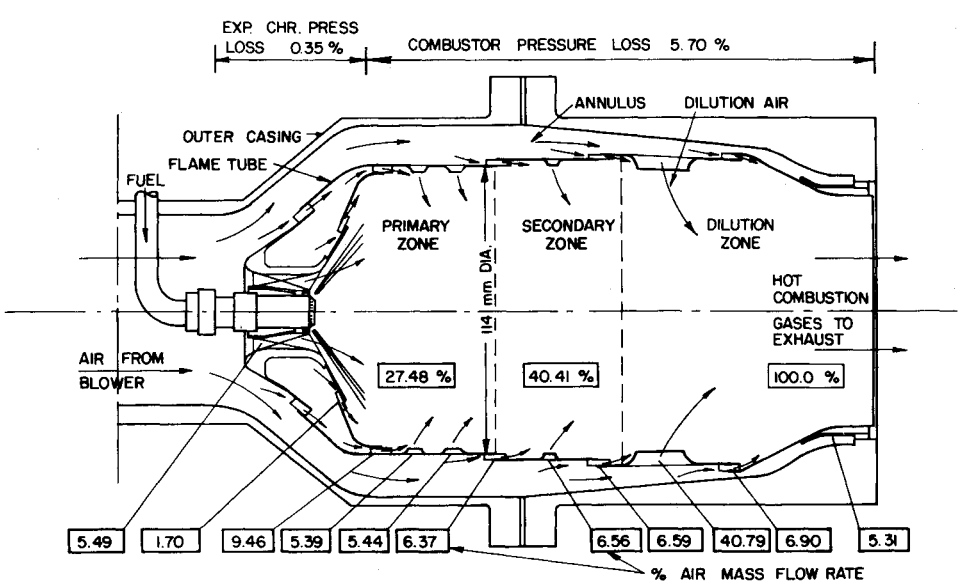

Fig. 1 Cross section through the combustor showing the air distribution.

Table 1 Sample test conditions

Test no.	Load	$\dot{M}_a$, kg/s	A/F	M_r	p_2, kPa	T_2, °C	T_{3m}, °C	$[(p_{02} - p_{03})/p_{02}]$, %	f = 227 Hz, Driver no. and $\dot{W}$ ① W	② W	③ W
27	One-quarter	0.0789	99.5	0.0143	89.5	57.3	ND 459 WD 460	0.60	——	——	150
25/150	One-quarter	0.0781	70.4	0.0143	88.9	57.4	ND 616 WD 619	0.75	——	——	150
31	One-quarter	0.0784	56.1	0.0142	89.5	56.6	ND 733 WD 735	0.72	——	——	150
35	One-quarter	0.0785	71.2	0.0144	88.7	57.6	ND 616 WD 619	0.66	——	147	153
42	One-quarter	0.0769	100.4	0.0141	88.9	58.7	ND 450 WD 453	0.61	149	149	156
36	One-quarter	0.0777	70.5	0.0142	88.8	57.2	ND 616 WD 620	0.67	147	147	156
37	One-quarter	0.0790	56.2	0.0141	90.7	55.7	ND 725 WD 734	0.72	148	148	157
32	One-half	0.1566	70.6	0.0278	91.1	57.8	ND 623 WD 626	2.19	——	——	150
34	Three-quarter	0.2485	70.7	0.0420	93.9	53.2	ND 528 WD 531	4.71	——	——	150
Theoretical full-load nominal		1.1657	60.4	0.0570	395.4	203	——	6.05	Standard combustor		
Stoichiometric		——	17.16	——	——	——	——	——		——	

Note: ND = no-drive, WD = with-drive.

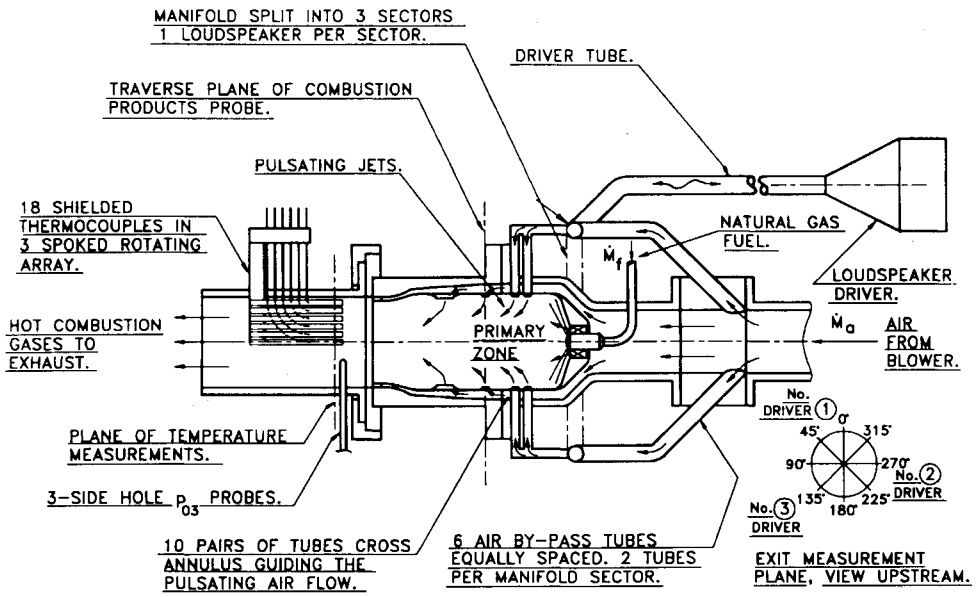

Fig. 2 Method for acoustic control of combustor primary zone air-jet mixing.

all thermocouples being positioned at different fixed radii, as shown in Fig. 3. Each local temperature measurement T_3 was the average of 11 samples, and the whole array of 432 measurements was averaged to define the exit plane mean temperature T_{3m}. The chromel-alumel thermocouples were accurate to ±2%, including random uncertainty, over the experimental range. The flame tube wall thermocouples were similar.

The air and fuel mass flow rates were accurate to ±2.5%, and ±1.5%, respectively. Individual static and stagnation pressure measurements were accurate to ±0.2%, whereas the hot pressure loss $p_{02} - p_{03}$ was measured to within ±4%.

Exit Plane Temperature Profile Measurements and Results

The objective of these measurements was to establish 1) that the temperature pattern was satisfactory, and typical, without acoustic drive; 2) that the temperature pattern was stable and repeatable for the selected conditions; and 3) the magnitude of changes in the temperature pattern caused by acoustic drive.

For comparative purposes, the data are presented in terms of the local average dimensionless relative temperature

$$\theta_m = [(T_3 - T_{3m})/(T_{3m} - T_2)] \tag{1}$$

The data may also be summarized in terms of the single mixing parameter

$$S_m = \left[\sum_1^n (T_3 - T_{3m})^2/(n-1)\right]^{1/2} \tag{2}$$

and the temperature profile acoustic driving effectiveness parameter

$$S_p = \left[\sum_1^n (T_{3WD} - T_{3ND})^2/n\right]^{1/2} \tag{3}$$

Both θ_m and S_m tend to zero as mixing is increased by the acoustic drive, while S_p maximizes. The "peakiness" of the

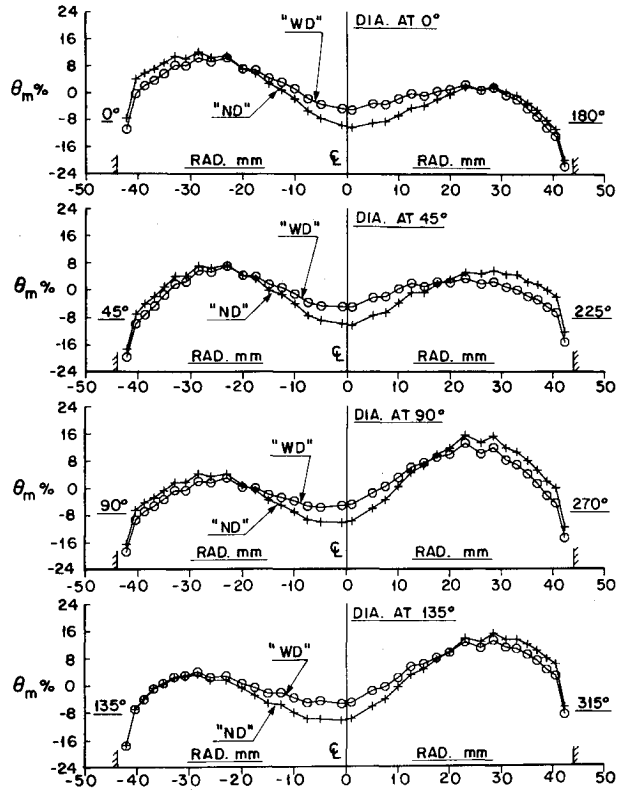

Fig. 3 Typical combustor exit plane diametral dimensionless temperature profiles, unsymmetrical driving, no. 3 driver 150 W, 227 Hz, one-quarter load, A/F = 70.4, no-drive Q = 16.4%, with-drive Q = 13.3%, test no. 25/150 (see Fig. 2 and Table 1).

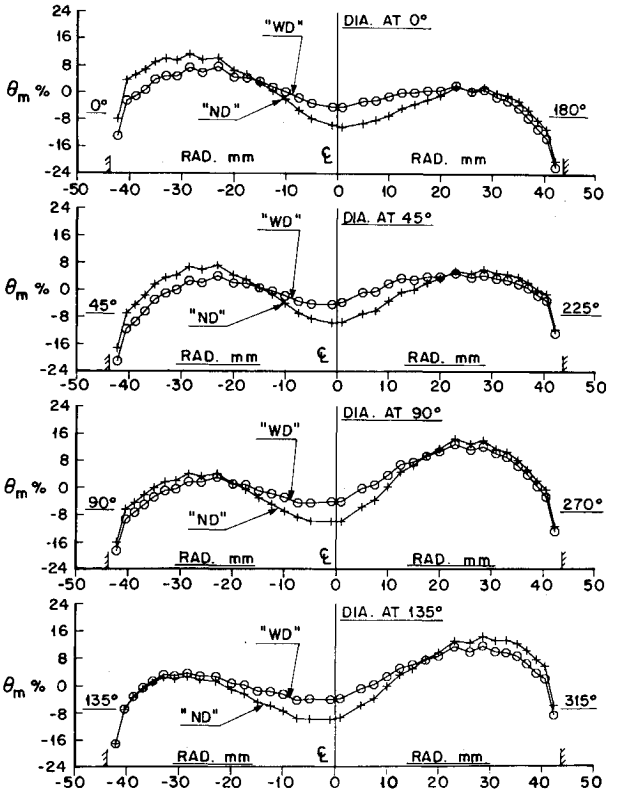

Fig. 4 Typical combustor exit plane diametral dimensionless temperature profiles, symmetrical driving, 3 drivers 150 W each, 227 Hz, one-quarter load, A/F = 70.5, no-drive Q = 15.1%, with-drive Q = 12.8%, test no. 36 (see Fig. 2 and Table 1).

temperature pattern was evaluated by the temperature pattern quality parameter

$$Q = [(T_{3\max} - T_{3m})/(T_{3m} - T_2)] \tag{4}$$

In order that differences between no-drive and with-drive conditions would not be masked by small-changes in running conditions, these values for a particular angular setting of the thermocouple array were obtained in pairs. That is, after obtaining a set of particular no-drive values, the acoustic drive was turned on, conditions allowed to stabilize, and then with-drive values recorded. The drive was then turned off and the array rotated to the next position followed by stabilization before the measurement procedure was repeated. As a check on steady operation, data at the 360-deg setting were obtained for comparison with the initial set at 0 deg.

When the data were analyzed, it was realized that the acoustic drive had little affect on the wall boundary-layer flows, and therefore, to avoid masking effects calculations of S_m and S_p were made on truncated data to eliminate the temperature boundary layer in the exit plane. To indicate this, these parameters have been designated as S_{mt} and S_{pt}. The chosen truncation radius of 38.8 mm was determined from the temperature boundary-layer thickness defined by the measured diametral temperature profiles and temperature contour maps.

Figure 3 presents typical exit plane diametral local average dimensionless temperature profiles for unsymmetrical driving by no. 3 driver at 7:30 o'clock position. The eight primary zone air-jets from the approximate 5 to 9 o'clock positions were strongly pulsed by the single driver at 150 W. Figure 4 shows similar plots for symmetrical equal driving of all primary zone air-jets by the three drivers at an average power of 150 W per acoustic driver. Table 1 shows a slight difference in individual driver powers caused by small differences in driver impedance, which is considered to be insignificant. The influence of driver power, air/fuel ratio, and air mass flow rate (load) was also investigated.

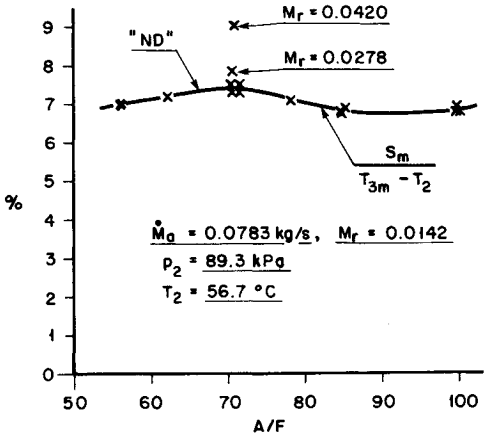

Fig. 5 No-drive dimensionless mixing parameter vs air/fuel ratio, untruncated data, one-quarter load, data at one-half and three-quarter loads shown for reference.

Test Results "No Acoustic Drive"

Visual comparison between Figs. 3 and 4 no-drive reveals very good repeatability between the tests. This is quantified by the mixing parameter, which has been plotted against A/F in Fig. 5 for all the data, and demonstrates that repeatability was within ±2% of the best fit line. Good similarity of temperature pattern was observed for all tests (a total of 14) at $M_r \cong 0.0143$ (one-quarter load) over the range of A/F values. But, as the load was increased to $M_r = 0.0420$ (three-quarter load), the cool central core in the pattern was flattened out. To check that the temperature pattern was stable

$$R = \left\{ \sum_{1}^{n} [(T_3)_{360} - (T_3)_0]^2/n \right\}^{1/2} \tag{5}$$

was calculated. This showed that the temperature pattern was stable to within $\pm 0.75\%$ in terms of $R/(T_{3m} - T_2)\%$. A similar calculation for the with-drive data showed the same stability tolerance. Stability of fuel mass flow rate, air mass flow rate, M_r, A/F, and the hot pressure loss ratio $(p_{02} - p_{03})/p_{02}$ during a test was on average within about $\pm 2.5\%$. Individual values, e.g., $\dot{M}_f$, could be as good as $\pm 0.2\%$.

Figure 6 gives the mixing S_{mt} for no-drive for truncated data vs A/F, and shows appreciable improvement in mixing for $A/F > 70$ as compared with the total data S_m calculations of Fig. 5. Mixing S_{mt} for no-drive improves with air mass flow rate or M_r as shown in Fig. 7, presumably due to flow turbulence increase.

The temperature pattern quality Q peaks at about 15.8% at $A/F = 70$ for no-drive, one-quarter load, and improves with loading, about 14% at three-quarter load. This is consistent with a full load design value of $Q = 15\%$ at $A/F = 60.4$.

Test Results "with Acoustic Drive"

Figures 3 and 4 show typical temperature changes due to strong acoustic drive, and despite the different driving arrangements, the temperature patterns were similar. The overall effect was to produce a more uniform temperature pattern. The affect of varying acoustic power was assessed for the unsymmetrical case of driving no. 3 driver alone, at one-quarter load, and $A/F = 70.9$, as for Fig. 3. Figure 8 shows the results in terms of S_{mt} and S_{pt}, which clearly shows a significant 31% improvement in mixing S_{mt}, although this saturated because the acoustic driving effectiveness S_{pt}, saturated at 3.1% for powers greater than 150 W. The rogue data point at 101 W appeared to be caused by combustor small aerodynamic instability at this power; several tests were run producing inconsistent results.

Varying the air/fuel ratio at one-quarter load with no. 3 driver at 150 W produced the data shown in Fig. 6, where comparison shows that mixing improves by 32% with-drive up to $A/F = 70$. Further richening resulted in poorer mixing, although still 9% better than no-drive, due to a sharp decline from 3.2 to 0.9% in acoustic driving effectiveness. Repeating these tests for all drivers at 151 W yielded the results of Fig. 9. In this case, the mixing with-drive improved steadily over that for no-drive, up to 35% as A/F was decreased. Effectively acoustic control maintained approximately the same mixing at all A/F values, which was brought about by acoustic driving effectiveness increasing with richening to 3.9%. Surprisingly, S_{pt} for three drivers at 151 W is only slightly greater than S_{pt} for one driver at 150 W for richening up to $A/F = 70$, and S_{mt} with-drive is almost identical. A single test, for drivers no. 2 and 3 at 150 W average each, therefore, is not surprisingly in close agreement as shown on Fig. 9.

As the loading was decreased (from three-quarter to one-quarter load) Fig. 7 shows that acoustic driving effectiveness increased in a manner sufficient to maintain approximately the same mixing with-drive at all loads tested. This was for no. 3 driver constant at 150 W, and A/F constant at 70.6. The curve fitted to the S_{pt} data has been constructed to vary inversely with $(\dot{M}_a)^{3/2}$, as will be discussed later.

The corresponding behavior of Q with-drive parallels that of S_{mt}. At one-fourth load, and $A/F = 70.9$, condition of

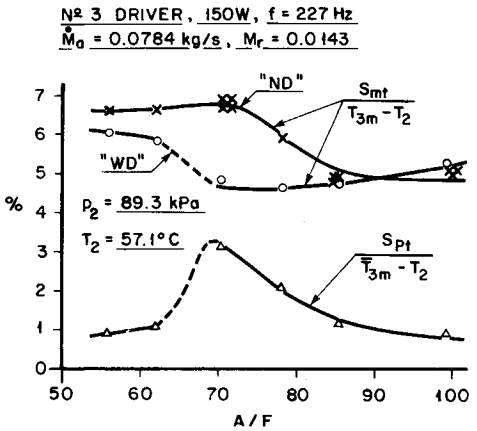

Fig. 6 Dimensionless mixing and driving effectiveness parameters vs A/F ratio, unsymmetrical driving at constant power, one-quarter load, truncated data.

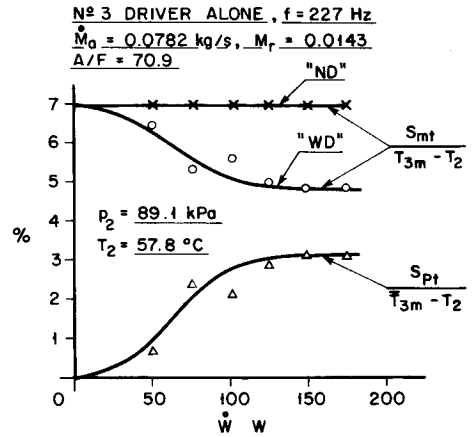

Fig. 8 Dimensionless mixing and driving effectiveness parameters vs driving power, unsymmetrical driving, one-quarter load, truncated data.

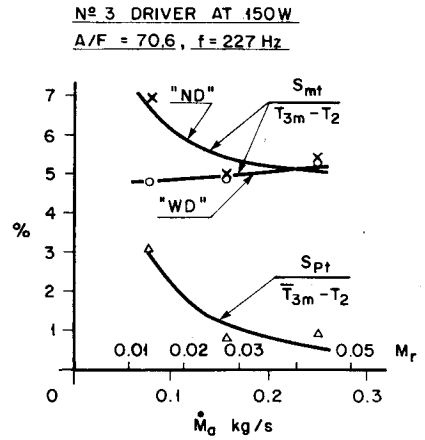

Fig. 7 Dimensionless mixing and driving effectiveness parameters vs air mass flow rate (load), unsymmetrical driving at constant power, truncated data.

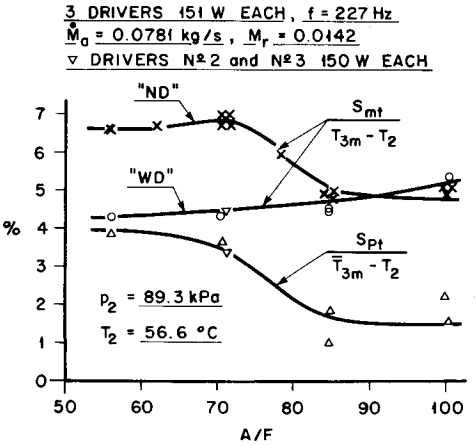

Fig. 9 Dimensionless mixing and driving effectiveness parameters vs A/F ratio, symmetrical driving at constant power, one-quarter load, truncated data.

greatest change, increasing driver power improved Q by up to 19% (150 W) for unsymmetrical driving by no. 3 driver alone. For one-fourth load, 151-W symmetrical driving, a 20% maximum improvement in Q with A/F richening was found at $A/F = 70$. And as driving effectiveness reduced with load increase up to three-quarter load, so did the improvement in Q, being only 5% for 150 W unsymmetrical driving at $A/F = 70.6$.

Table 1 shows a small consistent increase in the exit plane mean temperature T_{3m} with-drive, a maximum increase of 1.3% was found for test no. 37 at one-quarter load and $A/F = 56.2$. This suggests that acoustic drive produced a slight richening in A/F.

Discussion

Temperature Pattern Measurements

The no-drive temperature pattern typified by Figs. 3 and 4, and those at other loads (not shown), compare favorably with those shown in Ref. 12 and are satisfactory and typical for this kind of combustor without acoustic drive. The no-drive mixing behavior of Fig. 5 is about 7% on average, whereas that for Ref. 12 is somewhat better at an average value of about 5%. The no-drive mixing for untruncated data worsens as load is increased for these tests and those of Ref. 12, but the Ref. 12 mixing is again better (about 6% vs 8% at one-half load). The reason for somewhat worse mixing may be due to the facts that a more powerful blower and a new flame tube (our best copy) are now used with respect to Ref. 12.

Figures 5 and 6 for no-drive clearly show the effect of removal of the thermal boundary layer by truncating the data, and reveals a stronger dependence by mixing (S_{mt} compare with S_m) on A/F. This appears to be quite reasonable since, as the mixture richens combustion is more vigorous, temperature changes are more pronounced, and mixing worsens until $A/F = 70$ is reached. Furthermore, Fig. 7 indicates no-drive mixing S_{mt} improves with increase in loading, whereas plotting untruncated data shows the opposite behavior in that mixing S_m worsens, presumably due to boundary-layer thickening by increased turbulence.

Masking also has a strong effect on the with-drive data, halving the change in mixing (S_{mt} to S_m) shown in Fig. 8, and totally obscuring the trend in S_{mt} of Fig. 6 for instance. In Figs. 6–9, the variation of S_p is closely identical to S_{pt}, as it should be since the thermal boundary layer is subtracted out when calculating S_p for the total data, and this also confirms that the truncation radius chosen for the S_{pt} calculation was correctly selected.

Comparing the temperature profiles shown in Figs. 3 and 4, for the same no-drive conditions, reveals closely similar with-drive patterns despite unsymmetrical vs symmetrical, 150 W per driver, action. This surprising behavior can be explained by referring to Figs. 6 and 9, where it will be observed that mixing with-drive S_{mt}, for richening to $A/F = 70$, is nearly constant and identical for the different driving conditions. In contrast, the no-drive mixing worsens strongly with richening to $A/F = 70$. Thus, it appears that the acoustic drive offsets the effect of increasing combustion intensity on the mixing level S_{mt}, and since the driving pattern has no effect, it is most likely that increased jet penetration by the acoustic drive, causing increased blockage, is the cause. Careful inspection of the with-drive data shows that all the with-drive temperature patterns are very similar, i.e., the acoustic drive is strong enough to maintain the lean no-drive temperature pattern over the richening effect. Richening beyond $A/F = 70$, for unsymmetrical driving (Fig. 6) breaks the with-drive blockage and the mixing S_{mt} worsens to nearly no-drive rich values. For symmetrical driving (Fig. 9) this does not occur, and indicates that the aerodynamics of the combustor primary zone are being maintained in their lean state, whereas the unbalanced effects of a single driver can only achieve this with richening to $A/F = 70$. Furthermore, the basic temperature pattern is not affected by the driving arrangements or by A/F effects showing that major changes in the primary zone aerodynamics do not occur. Paradoxically, it is the no-drive mixing S_{mt} behavior with A/F richening that appears to control the acoustic driving effectiveness S_{pt}, since this is effectively the difference between with-drive and no-drive S_{mt} as Figs. 6 and 9 demonstrate. However, Fig. 8 shows that S_{mt} and S_{pt} depend on acoustic driving power, showing that there is acoustic control between the no-drive and with-drive mixing curves of Figs. 6 and 9 until full blockage or saturation occurs at about 150 W per driver. Figures 6 and 9 show that symmetrical driving produces slightly stronger effects than one driver alone. Also despite blockage being the dominant factor, the slightly improving with-drive mixing curves with richening suggest that the improved mixing by the modulated air jets has some effect.

Figure 7 and the effects of loading are now discussed. As the air mass flow rate is increased, the velocity of the primary zone air jets increase proportionately. Also, according to Ref. 17

$$(U_e/U_j)\alpha[(\dot{W}/\rho_j D^2 U_j^3)]^{1/2} \tag{6}$$

i.e., for a given jet and constant acoustic driver power, the pulsation strength U_e/U_j is inversely proportional to $(U_j)^{3/2}$. Therefore, the acoustic driving effectiveness should vary in a similar way with load, which is demonstrated by Fig. 7 where the S_{pt} curve was constructed in this manner. However, the no-drive S_{mt} curve ($A/F = 70.6$) has also reduced with load increase, and if the lean S_{mt} values did not correspondingly reduce with load, then this would contribute to the reduction in S_{pt}. Thus, the agreement of S_{pt} reduction with decrease in pulsation strength with load increase is perhaps fortuitous. Clearly, considerably more data is required before a full understanding is possible, and particularly for increased driving power. This was not tried because of amplifier-loudspeaker power limitation, because if U_j increase was the only factor, an eight times increase in $\dot{W}$ would be required at one-half load. Such a power increase is practical with appropriate apparatus modifications.

The temperature pattern quality behavior parallels that of mixing S_{mt} of Figs. 6–9, and for similar reasons. In general, acoustic drive improves the quality, which, depending on conditions, can be as much as 20% improvement.

Exit Plane Mean Temperature Measurements

Table 1 gives the exit plane mean temperature values for no-drive and with-drive conditions. This allows the no-drive mean temperature rise values $T_{3m} - T_2$ to be compared with those given in Refs. 12 and 13; the agreement is very good and shows that the combustor behaved normally. Inspection of Table 1 will reveal that there is always a small increase in T_{3m} with-drive, on average about 0.5% at one-quarter load. This is equivalent to an average change in A/F of -0.7%, which agrees with -0.5% measured at one-quarter load, and also there was an average change with-drive in air mass flow rate of -0.5%. Since the fuel mass flow rate on average was constant to within 0.1%, then the change in A/F was due to that in $\dot{M}_a$, and is evidence of flow blockage by the acoustic drive.

Driving Power Requirements

The energy conversion rate of the combustor at one-quarter load rich conditions is about 75 kW, therefore, the 0.45 kW driving power used for effective acoustic control is insignificant. No meaningful estimate of driving power required for significant acoustic control at full load conditions can be made because of the lack of data at one-half and three-quarter load conditions.

Conclusions

A small tubular combustor of conventional gas turbine design and behavior, employing acoustically controlled primary zone air-jet mixing processes, has been successfully tested at scaled one-quarter-load operating conditions, and some data were obtained at one-half and three-quarter loads. The acoustic drive produced a more uniform exit plane temperature pattern, resulting in up to 35% improvement in mixing relative to no-drive, and in up to 20% relative improvement in the temperature pattern quality. The effects depended on air/fuel ratio and, in general, improved relative to no-drive with richening. The acoustic driving effectiveness also improved with richening for a maximum value of 3.9% (28°C) of the mean temperature rise. Increasing the loading to three-quarter load, 150 W single driver power, reduced the acoustic driving effectiveness by about 80% with correspondingly reduced improvements in mixing and quality. Whether driving effectiveness could be regained by increased driving power was not resolved.

The effects of acoustic drive were controllable by means of the driving power, but saturated at about 150 W when a single acoustic driver was used. Increased flow blockage, caused by increased jet penetration by the acoustic drive, appears to be the control mechanism and did not depend on the driving pattern. However, symmetrical driving produced slightly stronger effects than one driver alone, and despite blockage being the dominant factor, there was evidence of slightly improved mixing due to jet modulation. Effectively acoustic control maintained the aerodynamics of the combustor primary zone in the lean state. Overall, acoustic control improved mixing and produced favorable general progressive control over the combustor exit plane temperature pattern. The maximum driving power used for effective acoustic control was insignificant in comparison with the energy conversion rate of the combustor.

Acknowledgments

The work was supported financially by the Natural Sciences and Engineering Research Council of Canada, under Grant No. A7801. Canadian Western Natural Gas Co. Ltd., generously supplied the natural gas for operation of the test rig. The authors are indebted to R. Bechtold, Chief Technical Supervisor, and particularly to Technicians W. Crews, C. Imer, G. East, and P. Halkett, for their expert work in the building of the test rig. We are also grateful to Research Technicians A. Moehrle and R. W. Gustafson for their invaluable assistance with instrumentation and operational requirements. This paper is dedicated to Thornton W. Price, of Arizona State University, Tempe, Arizona, in memory of his introduction of the first author to this area, for his unselfish encouragement in its later development, and sincere friendship.

References

[1]Lefebvre, A. W., "Ch. 4 Aerodynamics," *Gas Turbine Combustion*, McGraw-Hill Series in Energy, Combustion, and Environment, New York, 1983, pp. 107–155.

[2]Hahnemann, Von, H., and Ehret, L., "Uber den Einfluss Starker Schallwellen auf eine Stationar Brennende Gasflamme," *Zeitschriff fur Technisch Physik*, Vol. 24, 1943, pp. 228–242.

[3]Anderson, A. B. C., "Structure and Velocity of the Periodic Vortex-Ring Flow Pattern of a Primary Pfeifenton (Pipe Tone) Jet," *Journal of the Acoustical Society of America*, Vol. 27, No. 6, 1955, pp. 1048–1053.

[4]Becker, H. A., and Massaro, T. A., "Vortex Evolution in a Round Jet," *Journal of Fluid Mechanics*, Vol. 31, Pt. 3, 1968, pp. 435–448.

[5]Crow, S. C., and Champagne, F. H., "Orderly Structure in Jet Turbulence," *Journal of Fluid Mechanics*, Vol. 48, Aug. 1971, pp. 547–591.

[6]Kibens, V., "Discrete Noise Spectrum Generated by an Acoustically Excited Jet," *AIAA Journal*, Vol. 18, No. 4, 1980, pp. 434–441.

[7]Sarohia, V., and Massier, P. F., "Experimental Results of Large-Scale Structures in Jet Flows and Their Relation to Jet Noise Production," *AIAA Journal*, Vol. 16, No. 8, 1978, pp. 831–835.

[8]Heavens, S. N., "Visualisation of the Acoustic Excitation of a Subsonic Jet," *Journal of Fluid Mechanics*, Vol. 100, Pt. 1, 1980, pp. 185–200.

[9]Binder, G., and Favre-Marinet, M., "Mixing Improvement in Pulsating Turbulent Jets," *ASME Symposium on Fluid Mechanics of Mixing*, Georgia Inst. of Technology, Atlanta, GA, 1973, pp. 167–172.

[10]Hill, W. G., and Greene, P. R., "Increased Turbulent Jet Mixing Rates Obtained by Self-Excited Acoustic Oscillations," *Transactions of the American Society of Mechanical Engineers, Journal of Fluids Engineering*, Vol. 99, No. 3, 1977, pp. 520–525.

[11]Bremhorst, K., and Harch, W. H., "The Mechanism of Jet Entrainment," *AIAA Journal*, Vol. 16, No. 10, 1978, pp. 1104, 1105.

[12]Vermeulen, P. J., Odgers, J., and Ramesh, V., "Acoustic Control of Dilution-Air Mixing in a Gas Turbine Combustor," *Transactions of the American Society of Mechanical Engineers, Journal of Engineering for Power*, Vol. 104, No. 4, 1982, pp. 844–852.

[13]Vermeulen, P. J., Odgers, J., and Ramesh, V., "Full Load Operation of Gas Turbine Combustor with Acoustically Controlled Dilution-Air Mixing," *International Journal of Turbo and Jet Engines*, Vol. 4, Nos. 1–2, 1987, pp. 139–147.

[14]Vermeulen, P. J., and Yu, W. K., "An Experimental Study of the Mixing by an Acoustically Pulsed Axisymmetrical Air-Jet," *International Journal of Turbo and Jet Engines*, Vol. 4, Nos. 3–4, 1987, pp. 225–237.

[15]Vermeulen, P. J., Ramesh, V., and Yu, W. K., "Measurements of Entrainment by Acoustically Pulsed Axisymmetric Air Jets," *Transactions of the American Society of Mechanical Engineers, Journal of Engineering for Gas Turbines and Power*, Vol. 108, No. 3, 1986, pp. 479–484.

[16]Vermeulen, P. J., Rainville, P., and Ramesh, V., "Measurements of the Entrainment Coefficient of Acoustically Pulsed Axisymmetric Free Air Jets," *Transactions of the American Society of Mechanical Engineers, Journal of Engineering for Gas Turbines and Power*, Vol. 114, No. 2, 1992, pp. 409–415.

[17]Vermeulen, P. J., Chin, C.-F., and Yu, W. K., "Mixing of an Acoustically Pulsed Air Jet with a Confined Crossflow," *Journal of Propulsion and Power*, Vol. 6, No. 6, 1990, pp. 777–783.

[18]Vermeulen, P. J., Grabinski, P., and Ramesh, V., "Mixing of an Acoustically Excited Air Jet with a Confined Hot Crossflow," *Transactions of the American Society of Mechanical Engineers, Journal of Engineering for Gas Turbines and Power*, Vol. 114, No. 1, 1992, pp. 46–54.